

# Studies on two interesting microporous polymeric clusters $\{[Et_4N]_2[MS_4Cu_4(CN)_4]\}_n$ ( $M = Mo$ or $W$ ) with three-dimensional open frameworks: synthesis, structural characterization, strong optical non-linearities and large optical limiting properties

Chi Zhang,<sup>ab</sup> Yinglin Song,<sup>\*a</sup> Yan Xu,<sup>b</sup> Hoongkun Fun,<sup>c</sup> Guangyu Fang,<sup>a</sup> Yuxiao Wang<sup>a</sup> and Xinquan Xin<sup>b</sup>

<sup>a</sup> State Key Laboratory of Applied Optics, Department of Physics, Harbin Institute of Technology, Harbin 150001, P. R. China

<sup>b</sup> State Key Laboratory of Coordination Chemistry, Department of Chemistry, Nanjing University, Nanjing 210093, P. R. China

<sup>c</sup> X-Ray Crystallography Unit, School of Physics, Universiti Sains Malaysia 11800, USM, Penang, Malaysia

Received 17th March 2000, Accepted 20th June 2000

Published on the Web 27th July 2000

Reactions combining stoichiometric amounts of  $(Et_4N)_2MS_4$  ( $M = Mo$  or  $W$ ) and  $CuCN$  (1:4) in pyridine afforded interesting three-dimensional cluster polymers with open frameworks  $\{[Et_4N]_2[MS_4Cu_4(CN)_4]\}_n$  ( $M = Mo$  **1** or  $W$  **2**). Crystal structure determination shows that the anionic  $MS_4Cu_4$  units bridged by cyanide produce three-dimensional channels running down the crystallographic  $a$  axis. An alternative way to view this framework is in terms of the diamond structure, where C has alternately been replaced by a  $MS_4Cu_4$  aggregate and C–C by two parallel cyanide bridging ligands. In these intersecting channels the shortest distances between Cu atoms along the  $b$  and  $c$  axes are 15.22 and 8.11 Å respectively. Non-linear optical properties of the two clusters were investigated first with an 8 ns pulsed laser at 532 nm. These two clusters exhibit large optical limiting performance with limiting threshold values of 0.28 for **1**, 0.15 J cm<sup>-2</sup> for **2** respectively. Both compounds show strong third-order NLO absorption effects ( $\alpha_2$   $1.5 \times 10^{-9}$  **1**,  $1.6 \times 10^{-9}$  m W<sup>-1</sup> **2**) and self-focusing performance ( $n_2$   $1.84 \times 10^{-16}$  **1**,  $1.22 \times 10^{-16}$  m<sup>2</sup> W<sup>-1</sup> **2**) in  $3.64 \times 10^{-5}$  **1** and  $2.93 \times 10^{-5}$  mol dm<sup>-3</sup> **2** DMF solution separately. The corresponding effective NLO susceptibilities  $\chi^{(3)}$  are  $4.58 \times 10^{-9}$  **1** and  $5.12 \times 10^{-9}$  esu **2** while the corresponding hyperpolarizabilities ( $\gamma_{(1)} = 1.15 \times 10^{-29}$  and  $\gamma_{(2)} = 1.26 \times 10^{-29}$  esu) are also reported.

## Introduction

Transition metal–sulfur cluster chemistry has been developing progressively<sup>1</sup> since these clusters which have interesting electronic, optical, structural and catalytic properties are of biological and industrial significance in advanced materials, biological processes and catalytic reactions.<sup>2–4</sup> Tremendous interest in these clusters has recently been aroused in the search for better materials with third-order non-linear optical (NLO) properties because of their potential applications not only in the protection of optical sensors and human eyes from high-intensity laser beams, but also in the development of optical signal detection techniques such as those utilized in optical computers and broad-band communications.<sup>5,6</sup> Previously, the discrete Mo(W)/S/Cu(Ag) clusters along with their third-order non-linear optical properties had extensively been investigated,<sup>2,5–9</sup> for this kind of cluster is found to be able to combine the advantages of both inorganic compounds with the involvement of heavy atoms and organic molecules with the facility of structural alteration.<sup>10</sup> Nevertheless, the molecular construction of the extended structure mirrors the subject of current research interest. The reported cluster polymers of the Mo(W)/S/Cu(Ag) system are polynuclear chain polymers  $\{[MoOS_3Cu_3(CN)(py)_3]\}_n$ ,  $\{[W_4Ag_5S_{16}][Nd(DMF)_8]\}_n$ ,  $\{[W_4Ag_4S_{16}][Ca(DMF)_6]_2\}_n$  and  $\{[M_3Ag_3S_{12}][Nd(DMF)_8]\}_n$  ( $M = Mo$  or  $W$ ),<sup>11</sup> dinuclear infinite chain clusters  $[AgMS_4(\gamma\text{-MepyH})]_n$ ,  $[AgMS_4(\alpha\text{-MepyH})]_n$ ,  $\{[MoS_4Ag]\}_n$ ,  $\{[H_3NC(CH_2OH)_3\cdot R][WS_4Ag]\}_n$  ( $R = 2DMF$  or  $H_2O$ ),  $[MS_4Ti]_n$ ,<sup>12</sup> tetranuclear open polymers  $\{[(CuNCS)_3WS_4]^{2-}\}_n$ ,<sup>13</sup> pentanuclear open polymers

$\{[(CuL)_4MoS_4]^{2-}\}_n$  ( $L = Br$  or  $NCS$ ),  $\{[Cu_4(NCS)_5MoS_4]^{2-}\}_n$ ,<sup>14</sup> and heptanuclear network polymers  $[MS_4Cu_6X_4(py)_4]_n$ .<sup>15</sup> Unfortunately, among these clusters only  $[MS_4Ti]_n$ ,  $\{[MoOS_3Cu_3(CN)(py)_3]\}_n$  and  $[MS_4Cu_6X_4(py)_4]_n$  proved to have good NLO properties. Furthermore, cluster polymers with a three-dimensional framework in the Mo(W)/S/Cu(Ag) system are so rare that the NLO properties of the three-dimensional cluster polymers are still unidentified.

Moreover, the recent intense pursuit of open crystalline assemblies extends across the gamut of inorganic metal clusters, co-ordination complexes, and organic molecules.<sup>16</sup> The extended motifs are held together either by strong metal–ligand bonding or by weaker forces such as hydrogen-bonding and  $\pi$ – $\pi$  interactions. The driving force behind this research is to create open-framework materials with cavities and channels that may be exploited for desired properties including shape- and size-selective catalysis, separations, sensors, molecular recognition and optical applications.<sup>17</sup>

In order further to develop the study in this active field and also to search for better NLO materials, we now present two interesting microporous heterothiobimetallic cluster polymers  $\{[Et_4N]_2[MS_4Cu_4(CN)_4]\}_n$  ( $M = Mo$  **1** or  $W$  **2**) with cyanide-bridged three-dimensional open frameworks and an original study on their NLO properties in the Mo(W)/S/Cu(Ag) system. These two cluster polymers are characterized by X-ray crystallographic determination. The results of Z-scan experiments show that they possess strong NLO absorptive abilities and effective self-focusing effects. Large optical limiting (OL) properties are also observed.

## Experimental

### General

All reactions and manipulations were conducted using standard Schlenk techniques under an atmosphere of nitrogen. The starting materials  $(\text{Et}_4\text{N})_2\text{MS}_4$  ( $\text{M} = \text{Mo}$  or  $\text{W}$ ) were obtained according to the literature.<sup>18</sup> The solvents were carefully dried and distilled prior to use and other chemicals were generally used as commercially available.

### Preparation

$\{[\text{Et}_4\text{N}]_2[\text{MoS}_4\text{Cu}_4(\text{CN})_4]\}_n$  **1**.  $\text{CuCN}$  (0.358 g, 4 mmol) was added to pyridine (20  $\text{cm}^3$ ) and the solution refluxed and stirred for *ca.* 30 min in an inert atmosphere. The system changed from colorless to yellow-green and a suspension was obtained. Then  $(\text{Et}_4\text{N})_2\text{MoS}_4$  (0.485 g, 1 mmol) was added. The reacting system immediately turned deep red as the suspended substance dissolved gradually and was stirred for 20 min. The resulting solution was subsequently filtered to afford a black-red filtrate, layered with *i*-PrOH (20  $\text{cm}^3$ ) and allowed to stand at room temperature for about a month. Black-red polyhedral crystals of cluster **1** with suitable quality for X-ray diffraction were obtained (0.59 g, yield 70% based on  $\text{Mo}$ ). Found: C, 28.62; H, 4.89; N, 9.86%. Calc. for  $\text{C}_{20}\text{H}_{40}\text{Cu}_4\text{MoN}_6\text{S}_4$  **1**: C, 28.50; H, 4.78; N, 9.97%. IR (KBr pellets,  $\text{cm}^{-1}$ ): 2122vs and 458vs.

$\{[\text{Et}_4\text{N}]_2[\text{WS}_4\text{Cu}_4(\text{CN})_4]\}_n$  **2**. The same procedure was employed to synthesize cluster **2** except using  $(\text{Et}_4\text{N})_2\text{WS}_4$  (0.573 g, 1 mmol) instead of  $(\text{Et}_4\text{N})_2\text{MoS}_4$ . Orange-red polyhedral crystals were obtained (0.220 g, yield 24% based on  $\text{W}$ ). Found: C, 25.62; H, 4.21; N, 9.23%. Calc. for  $\text{C}_{20}\text{H}_{40}\text{Cu}_4\text{WN}_6\text{S}_4$  **2**: C, 25.80; H, 4.33; N, 9.03%. IR (KBr pellets,  $\text{cm}^{-1}$ ): 2122vs and 447vs.

### Crystal structure determinations

A well developed single crystal of cluster **1** or **2** with suitable dimensions was mounted on a glass fiber and diffraction data were collected on a Siemens Smart CCD area-detecting diffractometer by using an  $\omega$ -scan technique. The data reductions were performed on a Silicon Graphics Indy workstation with Smart-CCD software. An empirical SADABS absorption correction was applied.<sup>31</sup> All the metal atoms and S atoms were obtained by direct methods and other non-hydrogen atoms were located from the Fourier difference maps. The structures were solved by direct methods and refined by full-matrix least squares on  $F^2$  using the SHELXTL-PC (Version 5.1) package.<sup>32</sup> All non-hydrogen atoms were refined anisotropically. The hydrogen atoms were placed in their calculated positions (C–H, 0.96 Å), assigned fixed isotropic thermal parameters (1.2 times for  $\text{CH}_2$  and 1.5 times for  $\text{CH}_3$  those of atoms to which they are attached) and allowed to ride on their respective parent atoms. Their contributions were included in the structure factor calculations. The cyanide is disordered in the crystal structure, and each cyanide position is occupied by C or N with the occupancy factors being 0.5/0.5. The data processing and structure refinement parameters are listed in Table 1.

CCDC reference number 186/2047.

See <http://www.rsc.org/suppdata/dt/b0/b002164o/> for crystallographic files in .cif format.

### Other measurements

Elemental analyses for carbon, hydrogen and nitrogen were performed on a Perkin-Elmer 240C elemental analyzer. Infrared spectra were recorded with a Nicolet FT-170SX Fourier transform spectrometer (KBr pellets), electronic spectra on a Shimadzu UV-3100 spectrophotometer.

**Optical.** A DMF solution of the cluster **1** or **2** was placed in a 5 mm quartz cuvette for optical limiting property measure-

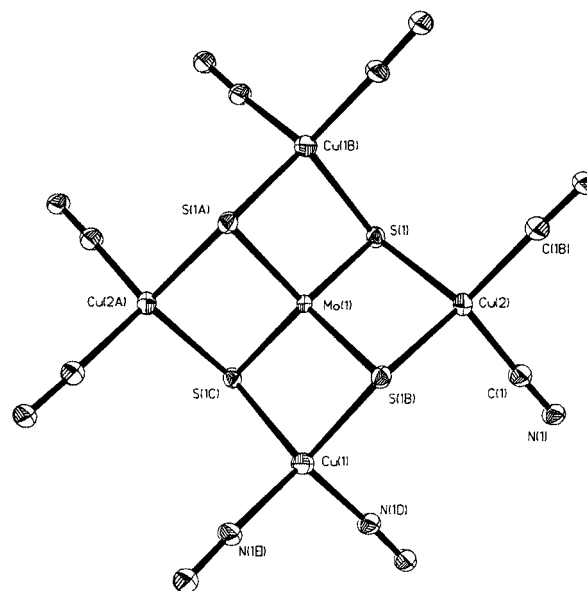


**Fig. 1** An ORTEP diagram of a section of the crystal structure of cluster polymer **1** (30% displacement ellipsoids). The cyanide C/N atoms are disordered and only one orientation is shown for simplicity.

ments which were performed with linearly polarized 8 ns pulses at 532 nm generated from a Q-switched frequency-doubled Nd:YAG laser. The clusters are stable toward air and laser light under experimental conditions. The spatial profiles of the optical pulses were of nearly Gaussian transverse mode. The pulsed laser was focused onto the sample cell with a 15 cm focal length mirror. The spot radius of the laser beam was measured to be 55  $\mu\text{m}$  (half-width at  $1/e^2$  maximum). The energies of the input and output pulses were measured simultaneously by precision laser detectors (Rjp-735 energy probes) while the incident energy was varied by a Newport Com. Attenuator. The interval between the laser pulses was chosen to be 1 s to avoid influence of thermal and long-term effects.

The effective third-order NLO absorptive and refractive properties of clusters **1** and **2** were recorded by moving the samples along the axis of the incident laser beam ( $Z$  direction) with respect to the focal point instead of being positioned at its focal point, and an identical set-up was adopted in the experiments to measure the  $Z$ -scan data. An aperture of 0.5 mm radius was placed in front of the detector to assist the measurement of the non-linear optical absorption and self-focusing effect.

## Results and discussion

### Crystal structure

Crystal structures of cluster polymers **1** and **2** have been determined by X-ray diffraction. They consist of one independent  $[\text{MS}_4(\text{CuCN})_4]^{2-}$  ( $\text{M} = \text{Mo}$  or  $\text{W}$ ) anion and two  $\text{Et}_4\text{N}^+$  cations. In both the  $[\text{Et}_4\text{N}]^+$  cations have their expected structure as well as normal distances and angles, which will not be discussed further. Selected bond distances and angles for **1** and **2** are collected in Table 2 and 3 respectively.

The structures of the anion  $[\text{MS}_4(\text{CuCN})_4]^{2-}$  in clusters **1** and **2** are isomorphous, and only that of **1** is described in detail with the ORTEP<sup>19</sup> diagram shown in Fig. 1, while the polymeric anion is constructed from  $\text{MoS}_4\text{Cu}_4$  units bridged by cyanide ligands. Each Mo atom of the structure is at the center of an essentially tetrahedral  $\text{MoS}_4$  unit in which the four Mo–S bond lengths are all quite similar to each other. Four edges of the  $\text{MoS}_4$  tetrahedron are co-ordinated by Cu atoms with Mo–Cu distances ranging from 2.7514(7) to 2.7785(7) Å,

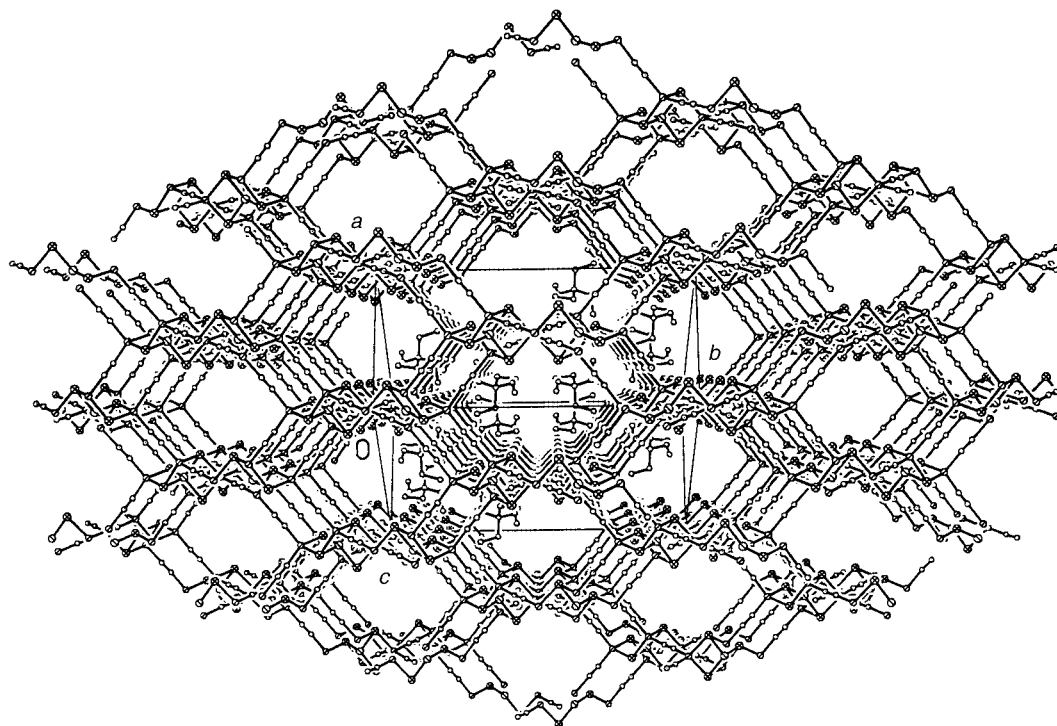


Fig. 2 Packing of cluster polymer 1 viewed along the *a* axis.

longer than the corresponding separations observed in other discrete  $[\text{MoS}_4(\text{CuX})_n]^{2-}$  ( $n = 1-4$ ) anions.<sup>20,21</sup> Within the  $\text{MoCu}_4$  core, five metal atoms are perfectly coplanar with a Cu–Mo–Cu angle concerning the two mutually *trans* Cu atoms of  $180^\circ$ , which leads to an ideal crystallographic  $D_{2d}$  symmetry for the  $\text{MoS}_4\text{Cu}_4$  aggregate. Two *cis* Cu atoms, Cu(1) and Cu(2), have a distorted-tetrahedral geometry with their tetrahedral apices occupied by two triply bridging S atoms and two cyanide bridging C or N atoms, forming a  $\text{CuS}_2\text{C}_2$ , a  $\text{CuS}_2\text{N}_2$  and  $\text{CuS}_2\text{CN}$  unit respectively. (The bridged cyanide is disordered, each position being occupied by C or N atom with occupancy 0.5/0.5.) These tetrahedra are mutually linked by bridged cyanide ligands thus constructing a polymeric three-dimensional anion of basic formula  $[\text{MoS}_4(\text{CuCN})_4]_n^{2-}$ . Comparing with the analogous cluster polymer  $[\text{WS}_4(\text{CuSCN})_4]_n^{2-}$  with bridging thiocyanate groups,<sup>21b,c</sup> which exhibits a significant deviation of Cu–NCS and Cu–SCN angles, the polymeric anions bridged by the cyanide are very slightly bent with Cu–C–N  $175.0(4)$  and Cu–N–C  $176.4(4)^\circ$ . The corresponding cyanide ligands are involved in inter-aggregate linear bridges between Cu atoms of the next  $\text{MoS}_4\text{Cu}_4$  unit, forming a three-dimensional open framework, and displaying no layering but particular directionality. The bond distances of Cu–N and Cu–C are  $1.983(4)$  and  $1.977(4)$  Å respectively, while the bond angles of  $\text{C}(1e)(x + \frac{1}{4}, y - \frac{1}{4}, -z + \frac{1}{2})\text{--Cu}(1)\text{--C}(1d)(-x - \frac{3}{4}, -y, -z + \frac{1}{2})$  and  $\text{N}(1b)(-x - \frac{5}{4}, y, -z + \frac{3}{4})\text{--Cu}(2)\text{--N}(1)$  are  $110.9(2)$  and  $110.5(2)^\circ$  separately. Owing to different co-ordination of Cu(1) and Cu(2) atoms, the Cu(2)–S(1) bond length ( $2.3272(10)$  Å) is slightly shorter than Cu(1)–S(1b)( $-x - \frac{5}{4}, y, -z + \frac{3}{4}$ ) ( $2.3416(11)$  Å).

The packing of the unit cell is depicted in Fig. 2. The units shown in Fig. 1 are fused together tetrahedrally, resulting in an anionic open framework containing a three-dimensional intersecting channel system, where the channels run parallel to the crystallographic directions of  $[100]$  and  $[010]$ . These channels are occupied by the  $\text{Et}_4\text{N}^+$  cations, which appear to induce the polymeric structure and to balance the cluster anions. An alternative way to view this framework, displayed in Fig. 3, is in terms of the diamond structure, where C has alternately been replaced by  $\text{MoS}_4\text{Cu}_4$  aggregates and the C–C

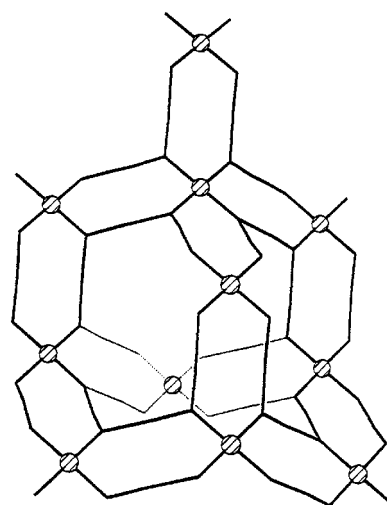


Fig. 3 An alternative way to view the structure of cluster polymer 1, which contains  $\text{MoS}_4\text{Cu}_4$  aggregates as building blocks linked by two parallel cyanide bridging ligands (⊗ represents the Mo atoms, other atoms omitted for clarity).

bonds by two parallel cyanide bridging ligands. However, unlike the diamond lattice, microporosity is created as a consequence of the larger size of the inorganic clusters compared to carbon atoms. In these intersecting channels the shortest distances between Cu atoms along the *b* and *c* axes are  $15.22$  and  $8.11$  Å respectively.

It is interesting that our previous efforts to prepare this kind of cluster polymer, especially Mo-containing compounds, have all been frustrated by using  $(\text{NH}_4)_2\text{MS}_4$  ( $\text{M} = \text{Mo}$  or  $\text{W}$ ) as starting materials in the same or different reaction system. This is partly attributed to the  $\text{NH}_4^+$  cations which have low solubility and too small volume to sustain the intersecting channels. The  $\text{Et}_4\text{N}^+$  cations can induce the polymeric structure and occupy the channels of the three-dimensional open framework as well as help to achieve the charge balance in the cluster polymers.

**Table 1** Crystal data for  $\{[\text{Et}_4\text{N}]_2[\text{MoS}_4\text{Cu}_4(\text{CN})_4]\}_n$  **1** and  $\{[\text{Et}_4\text{N}]_2[\text{WS}_4\text{Cu}_4(\text{CN})_4]\}_n$  **2**

Chemical formula	$\text{C}_{20}\text{H}_{40}\text{Cu}_4\text{MoN}_6\text{S}_4$	$\text{C}_{20}\text{H}_{40}\text{Cu}_4\text{N}_6\text{S}_4\text{W}$
Formula weight	842.92	930.83
Crystal system	Orthorhombic	Orthorhombic
Space group	$F_{ddd}$	$F_{ddd}$
$\mu(\text{Mo-K}\alpha)/\text{mm}^{-1}$	3.552	7.086
$a/\text{\AA}$	10.9696(2)	10.8968(1)
$b/\text{\AA}$	23.0792(5)	23.0553(3)
$c/\text{\AA}$	23.3276(6)	23.2870(1)
$V/\text{\AA}^3$	5905.8(2)	5850.37(10)
$Z$	8	8
Temperature of data collection/K	293(2)	293(2)
Reflections collected/unique	8147/1838 [ $R_{\text{int}} = 0.0619$ ]	10354/1975 [ $R_{\text{int}} = 0.0545$ ]
Final $R$ indices [ $I > 2\sigma(I)$ ]	$R_1 = 0.0435$ , $wR = 0.1215$	$R_1 = 0.0347$ , $wR = 0.0896$

**Table 2** Selected bond lengths ( $\text{\AA}$ ) and angles ( $^\circ$ ) of  $\{[\text{Et}_4\text{N}]_2[\text{MoS}_4\text{Cu}_4(\text{CN})_4]\}_n$  **1**

Mo(1)–S(1c)	2.2159(9)	Cu(2)–N(1)	1.983(4)
Mo(1)–S(1b)	2.2159(9)	Cu(1)–S(1b)	2.3416(11)
Mo(1)–S(1a)	2.2159(9)	Cu(1)–S(1c)	2.3416(11)
Mo(1)–S(1)	2.2159(9)	Cu(1)–C(1e)	1.977(4)
Mo(1)–Cu(2a)	2.7514(7)	Cu(1)–C(1d)	1.977(4)
Mo(1)–Cu(1)	2.7785(7)	Cu(2)–S(1)	2.3272(10)
Mo(1)–Cu(1b)	2.7785(7)	Cu(2)–S(1b)	2.3272(10)
Cu(2)–N(1b)	1.983(4)	S(1)–Cu(1b)	2.3416(11)
		C(1)–Cu(1d)	1.977(4)
S(1c)–Mo(1)–S(1b)	109.04(5)	Cu(1)–Mo(1)–Cu(1b)	180.0
S(1c)–Mo(1)–S(1a)	109.19(5)	N(1b)–Cu(2)–N(1)	110.5(2)
S(1b)–Mo(1)–S(1a)	110.19(5)	N(1b)–Cu(2)–S(1)	108.26(12)
S(1c)–Mo(1)–S(1)	110.19(5)	N(1)–Cu(2)–S(1)	113.93(13)
S(1b)–Mo(1)–S(1)	109.19(5)	N(1b)–Cu(2)–S(1b)	113.93(13)
S(1a)–Mo(1)–S(1)	109.04(5)	N(1)–Cu(2)–S(1b)	108.26(12)
S(1c)–Mo(1)–Cu(2a)	54.59(2)	S(1)–Cu(2)–S(1b)	101.81(5)
S(1b)–Mo(1)–Cu(2a)	125.41(2)	N(1b)–Cu(2)–Mo(1)	124.75(12)
S(1a)–Mo(1)–Cu(2a)	54.59(2)	N(1)–Cu(2)–Mo(1)	124.75(12)
S(1)–Mo(1)–Cu(2a)	125.41(2)	S(1)–Cu(2)–Mo(1)	50.90(3)
S(1c)–Mo(1)–Cu(2)	125.41(2)	S(1b)–Cu(2)–Mo(1)	50.90(3)
S(1b)–Mo(1)–Cu(2)	54.59(2)	C(1e)–Cu(1)–C(1d)	110.9(2)
S(1a)–Mo(1)–Cu(2)	125.41(2)	C(1e)–Cu(1)–S(1b)	112.92(13)
S(1)–Mo(1)–Cu(2)	54.59(2)	C(1d)–Cu(1)–S(1b)	109.46(12)
Cu(2a)–Mo(1)–Cu(2)	180.0	C(1e)–Cu(1)–S(1c)	109.46(12)
S(1c)–Mo(1)–Cu(1)	54.52(3)	C(1d)–Cu(1)–S(1c)	112.92(13)
S(1b)–Mo(1)–Cu(1)	54.52(3)	S(1b)–Cu(1)–S(1c)	100.82(5)
S(1a)–Mo(1)–Cu(1)	125.48(3)	C(1e)–Cu(1)–Mo(1)	124.53(12)
S(1)–Mo(1)–Cu(1)	125.48(3)	C(1d)–Cu(1)–Mo(1)	124.53(12)
Cu(2a)–Mo(1)–Cu(1)	90.0	S(1b)–Cu(1)–Mo(1)	50.41(3)
Cu(2)–Mo(1)–Cu(1)	90.0	S(1c)–Cu(1)–Mo(1)	50.41(3)
S(1c)–Mo(1)–Cu(1b)	125.48(3)	Mo(1)–S(1)–Cu(2)	74.50(3)
S(1b)–Mo(1)–Cu(1b)	125.48(3)	Mo(1)–S(1)–Cu(1b)	75.07(3)
S(1a)–Mo(1)–Cu(1b)	54.52(3)	Cu(2)–S(1)–Cu(1b)	113.76(4)
S(1)–Mo(1)–Cu(1b)	54.52(3)	N(1)–C(1)–Cu(1d)	175.0(4)
Cu(2a)–Mo(1)–Cu(1b)	90.0	C(1)–N(1)–Cu(2)	176.4(4)
Cu(2)–Mo(1)–Cu(1b)	90.0		

Symmetry transformations used to generate equivalent atoms: a  $-x - \frac{5}{4}, -y - \frac{1}{4}, z$ ; b  $-x - \frac{5}{4}, y, -z + \frac{3}{4}$ ; c  $x, -y - \frac{1}{4}, -z + \frac{3}{4}$ ; d  $-x - \frac{3}{2}, -y, -z + \frac{1}{2}$ ; e  $x + \frac{1}{4}, y - \frac{1}{4}, -z + \frac{1}{2}$ .

**Table 3** Selected bond lengths ( $\text{\AA}$ ) and angles ( $^\circ$ ) of  $\{[\text{Et}_4\text{N}]_2[\text{WS}_4\text{Cu}_4(\text{CN})_4]\}_n$  **2**

W(1)–S(1c)	2.2050(9)	Cu(1)–N(1e)	1.964(4)
W(1)–S(1)	2.2050(9)	Cu(1)–S(1b)	2.3522(11)
W(1)–S(1a)	2.2050(9)	Cu(1)–S(1c)	2.3522(11)
W(1)–S(1b)	2.2050(9)	Cu(2)–C(1b)	1.964(4)
W(1)–Cu(2)	2.7637(7)	Cu(2)–C(1)	1.964(4)
W(1)–Cu(2a)	2.7637(7)	Cu(2)–S(1)	2.3344(10)
W(1)–Cu(1b)	2.7925(8)	Cu(2)–S(1b)	2.3344(10)
W(1)–Cu(1)	2.7925(8)	S(1)–Cu(1b)	2.3522(11)
Cu(1)–N(1d)	1.964(4)	N(1)–Cu(1d)	1.964(4)
S(1c)–W(1)–S(1)	109.83(5)	Cu(1b)–W(1)–Cu(1)	180.0
S(1c)–W(1)–S(1a)	109.31(5)	N(1d)–Cu(1)–N(1e)	112.0(2)
S(1)–W(1)–S(1a)	109.28(5)	N(1d)–Cu(1)–S(1b)	109.31(13)
S(1c)–W(1)–S(1b)	109.28(5)	N(1e)–Cu(1)–S(1b)	112.99(13)
S(1)–W(1)–S(1b)	109.31(5)	N(1d)–Cu(1)–S(1c)	112.99(13)
S(1a)–W(1)–S(1b)	109.83(5)	N(1e)–Cu(1)–S(1c)	109.31(13)
S(1c)–W(1)–Cu(2)	125.34(2)	S(1b)–Cu(1)–S(1c)	99.72(5)
S(1)–W(1)–Cu(2)	54.66(2)	N(1d)–Cu(1)–W(1)	124.01(12)
S(1a)–W(1)–Cu(2)	125.34(2)	N(1e)–Cu(1)–W(1)	124.01(12)
S(1b)–W(1)–Cu(2)	54.66(2)	S(1b)–Cu(1)–W(1)	49.86(3)
S(1c)–W(1)–Cu(2a)	54.66(2)	S(1c)–Cu(1)–W(1)	49.86(3)
S(1)–W(1)–Cu(2a)	125.34(2)	C(1b)–Cu(2)–C(1)	111.3(2)
S(1a)–W(1)–Cu(2a)	54.66(2)	C(1b)–Cu(2)–S(1)	108.44(12)
S(1b)–W(1)–Cu(2a)	125.34(2)	C(1)–Cu(2)–S(1)	113.75(13)
Cu(2)–W(1)–Cu(2a)	180.0	C(1b)–Cu(2)–S(1b)	113.75(13)
S(1c)–W(1)–Cu(1b)	125.36(3)	C(1)–Cu(2)–S(1b)	108.44(12)
S(1)–W(1)–Cu(1b)	54.64(3)	S(1)–Cu(2)–S(1b)	100.79(5)
S(1a)–W(1)–Cu(1b)	54.64(3)	C(1b)–Cu(2)–W(1)	124.34(12)
S(1b)–W(1)–Cu(1b)	125.36(3)	C(1)–Cu(2)–W(1)	124.34(12)
Cu(2)–W(1)–Cu(1b)	90.0	S(1)–Cu(2)–W(1)	50.40(3)
Cu(2a)–W(1)–Cu(1b)	90.0	S(1b)–Cu(2)–W(1)	50.40(3)
S(1c)–W(1)–Cu(1)	54.64(3)	W(1)–S(1)–Cu(2)	74.95(3)
S(1)–W(1)–Cu(1)	125.36(3)	W(1)–S(1)–Cu(1b)	75.50(3)
S(1a)–W(1)–Cu(1)	125.36(3)	Cu(2)–S(1)–Cu(1b)	113.93(4)
S(1b)–W(1)–Cu(1)	54.64(3)	C(1)–N(1)–Cu(1d)	174.4(4)
Cu(2)–W(1)–Cu(1)	90.0	N(1)–C(1)–Cu(2)	175.8(4)
Cu(2a)–W(1)–Cu(1)	90.0		

Symmetry transformations used to generate equivalent atoms: a  $-x - \frac{5}{4}, -y - \frac{1}{4}, z$ ; b  $-x - \frac{5}{4}, y, -z + \frac{3}{4}$ ; c  $x, -y - \frac{1}{4}, -z + \frac{3}{4}$ ; d  $-x - \frac{3}{2}, -y, -z + \frac{1}{2}$ ; e  $x + \frac{1}{4}, y - \frac{1}{4}, -z + \frac{1}{2}$ .

### Infrared spectra and electronic spectra

The IR spectra of  $\{[\text{Et}_4\text{N}]_2[\text{MS}_4\text{Cu}_4(\text{CN})_4]\}_n$  ( $M = \text{Mo}$  or  $\text{W}$ ) exhibit characteristic strong bands at 458 **1** and 447  $\text{cm}^{-1}$  **2** assigned to the  $\mu_3\text{-S}$  stretching vibration of the  $\text{MS}_4$  group, while the very strong absorption at 2122  $\text{cm}^{-1}$  is attributed to the characteristic stretch vibration of the  $\text{CN}^-$  group.

The similarity in the structures of the two clusters also leads to similar electronic spectra, which is confirmed by Fig. 4. The red shift in the spectrum of **1** is expected since it contains one Mo instead of one W atom. The first absorption peaks of the two clusters located at 521 **1** and 443 nm **2**, can be assigned as charge-transfer bands of the type  $(\pi)\text{S} \rightarrow (\text{d})\text{M}$  ( $M = \text{Mo}$  or  $\text{W}$ ) arising from the  $\text{MS}_4$  moiety and both are red-shifted compared to those of the free  $[\text{MS}_4]^{2-}$  anion (472 nm for Mo and 397 nm for W).<sup>18</sup> It is noticed that electronic spectra of the

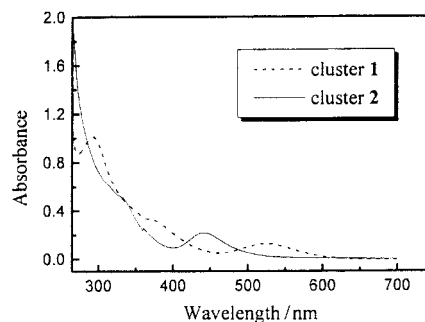


**Fig. 4** Electronic spectra of  $\{[\text{Et}_4\text{N}]_2[\text{MoS}_4\text{Cu}_4(\text{CN})_4]\}_n$  **1** and  $\{[\text{Et}_4\text{N}]_2[\text{WS}_4\text{Cu}_4(\text{CN})_4]\}_n$  **2** in DMF solution with 1 cm optical path. The cluster concentrations are  $1.0 \times 10^{-5} \text{ mol dm}^{-3}$ .

two clusters show relatively low linear absorption in the visible and near-infrared regions, promising low intensity loss and little temperature change caused by photon absorption when light propagates in the materials.

### Non-linear optical properties

Although the NLO properties of the discrete Mo(W)/S/Cu(Ag) cluster compounds had extensively been explored, the only cluster polymers possessing good NLO performance are the one-dimensional chain clusters  $\{[\text{Bu}_4\text{N}][\text{MS}_4\text{TI}]\}_n$  ( $\text{M} = \text{Mo}$  or  $\text{W}$ ),<sup>12d</sup>  $\{[\text{MoOS}_3\text{Cu}_3(\text{CN})(\text{py})_3] \cdot 0.5\text{C}_6\text{H}_6\}_n$ <sup>11a</sup> and the two-dimensional network cluster  $[\text{MoS}_4\text{Cu}_6\text{I}_4(\text{py})_4]_n$ .<sup>15</sup> In this study we have found that three-dimensional cluster polymers  $\{[\text{Et}_4\text{N}]_2[\text{MS}_4\text{Cu}_4(\text{CN})_4]\}_n$  ( $\text{M} = \text{Mo}$  **1** or **2**), are the first examples to exhibit strong NLO absorptive and refractive effects as well as large OL abilities. The NLO properties and the OL performance were investigated with 532 nm laser pulses of 8 ns duration in  $3.64 \times 10^{-5}$  and  $2.93 \times 10^{-5}$  mol dm<sup>-3</sup> DMF solution for **1** and **2** respectively.<sup>22</sup>

The non-linear absorption components of clusters **1** and **2** were evaluated by Z-scan experiment under an open-aperture configuration (Figs. 5a, 6a). The NLO absorption data obtained under the conditions used in this study can be well described by eqn. (1),<sup>22a,b</sup> which describes a third-order NLO

$$T(z) = \frac{1}{\sqrt{\pi}q(z)} \int_{-\infty}^{\infty} \ln[1 + q(z)]e^{-\tau^2} d\tau$$

$$q(z) = a_2^{\text{eff}} I(z) \frac{1 - e^{-a_0 L}}{a_0} \quad (1)$$

absorptive process, where  $a_0$  and  $a_2$  are linear and effective third-order NLO absorptive coefficients,  $\tau$  is the time, and  $L$  is the optical path. Light transmittance ( $T$ ) is a function of the sample's  $Z$  position (with respect to the focal point at  $Z = 0$ ). The solid lines in Figs. 5(a) and 6(a) are the theoretical curves from eqn. (1).

The non-linear refractive properties of clusters **1** and **2** were assessed by dividing the normalized Z-scan data obtained under the closed-aperture configuration by the normalized Z-scan data obtained under the open-aperture configuration (Figs. 5b, 6b). This procedure helps to extract information on NLO refraction from a raw data set containing mixed information on both refraction and absorption.<sup>22</sup> An effective third-order non-linear refractive index  $n_2$  can be derived from the difference between normalized transmittance values at valley and peak positions ( $\Delta T_{v-p}$ ) by using eqn. (2) with measured values  $\Delta T_{v-p} = 1.23$  **1** and 1.12 **2**.

$$n_2^{\text{eff}} = \frac{\lambda a_0}{0.812\pi I(1 - e^{-a_0 L})} \Delta T_{v-p} \quad (2)$$

A reasonably good fit between the experimental data and theoretical curve was obtained, which suggests that the experimentally obtained NLO effects are effectively third order in nature. The effective  $a_2$  values of  $1.5 \times 10^{-9}$  **1**,  $1.6 \times 10^{-9}$  m W<sup>-1</sup> **2** and  $n_2$  values of  $1.84 \times 10^{-16}$  **1**,  $1.22 \times 10^{-16}$  m<sup>2</sup> W<sup>-1</sup> **2** respectively were derived for the samples from the theoretical curves. In comparison with other discrete clusters and cluster polymers, the non-linear absorptive index  $a_2$  of clusters **1** and **2** are comparable to those of  $[\text{Mo}_2\text{Ag}_4\text{S}_8(\text{PPh}_3)_4]$ ,<sup>6a</sup>  $[\text{W}_2\text{Ag}_4\text{S}_8(\text{AsPh}_3)_4]$ <sup>5b</sup> and  $[\text{MoS}_4\text{Cu}_6\text{I}_4(\text{py})_4]$ ,<sup>15</sup> which have the largest values known, and superior to those of other inorganic clusters. It should be emphasized that the Z-scan results here could not reveal the origins of the observed non-linearities. Both excited state population (or absorption) and two-photon absorption can be responsible for these measured NLO effects.

In accordance with the observed  $a_2$  and  $n_2$  values, the modulus of the effective third-order susceptibility  $\chi^{(3)}$  can be calculated by eqn. (3), where  $\nu$  is frequency of the laser light,

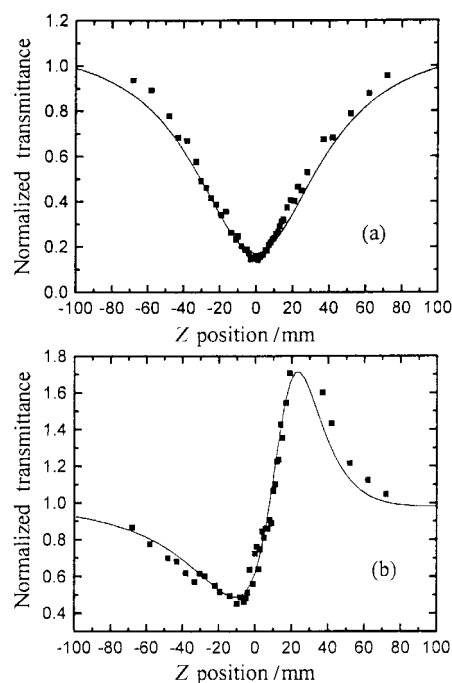


**Fig. 5** Z-scan data of  $\{[\text{Et}_4\text{N}]_2[\text{MoS}_4\text{Cu}_4(\text{CN})_4]\}_n$  in  $3.64 \times 10^{-5}$  mol dm<sup>-3</sup> DMF solution at 532 nm with  $I_0$  being  $8.2 \times 10^{12}$  W m<sup>-2</sup>: (a) collected under the open aperture configuration showing NLO absorption; (b) obtained by dividing the normalized Z-scan data obtained under closed aperture configuration by the normalized Z-scan data in (a) (shows the self-focusing effect of cluster **1**). The solid curves are the theoretical fit, based on eqns. (1) and (2).

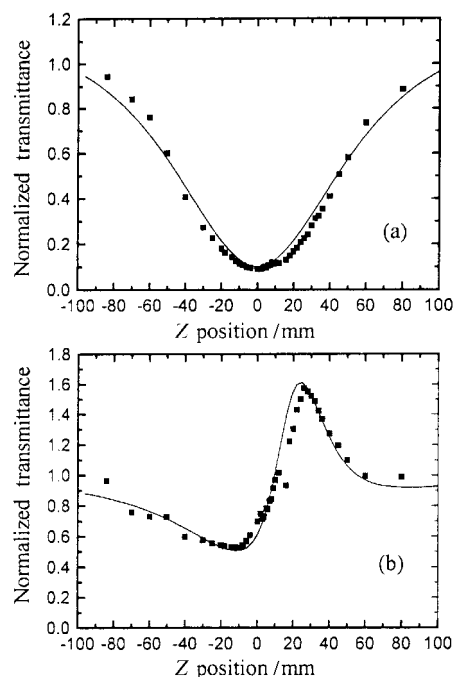


**Fig. 6** Z-scan data of  $\{[\text{Et}_4\text{N}]_2[\text{WS}_4\text{Cu}_4(\text{CN})_4]\}_n$  in  $2.93 \times 10^{-5}$  mol dm<sup>-3</sup> DMF solution at 532 nm with  $I_0$   $8.2 \times 10^{12}$  W m<sup>-2</sup>. Details as in Fig. 5.

$$|\chi^{(3)}| = \sqrt{\left(\frac{9 \times 10^8 \epsilon_0 n_0^2 c^2}{2\nu} a_2\right)^2 + \left(\frac{cn_0^2}{80\pi} n_2\right)^2} \quad (3)$$

$n_0$  is the linear refractive index of the sample,  $\epsilon_0$  and  $c$  are the permittivity and the speed of light in a vacuum, respectively. For  $3.64 \times 10^{-5}$  mol dm<sup>-3</sup> **1** and  $2.93 \times 10^{-5}$  mol dm<sup>-3</sup> **2** DMF solution, the  $\chi^{(3)}$  values were calculated to be  $4.58 \times 10^{-9}$  **1** and  $5.12 \times 10^{-9}$  esu **2**. The corresponding modulus of the hyperpolarizabilities  $\gamma$  of  $1.15 \times 10^{-29}$  **1** and  $1.26 \times 10^{-29}$  esu **2** was obtained from  $\chi^{(3)} = \gamma NF^4$ , where  $N$  is the number density of the

**Table 4** Non-linear optical properties of compounds measured at 532 nm with ns laser pulses

Compound	Structure type	$a_2/m\text{ W}^{-1}$	$n/m^2\text{ W}^{-1}$	$\chi^3/\text{esu}$	$N/\text{mol dm}^{-3}$	Ref.
[WOS <sub>3</sub> Cu <sub>2</sub> (PPh <sub>3</sub> ) <sub>4</sub> ]	Butterfly	$<10^{-12}$	$8 \times 10^{-18}$	$2 \times 10^{-11}$	$1.2 \times 10^{-4a}$	5(c)
[MoOS <sub>3</sub> Cu <sub>2</sub> (PPh <sub>3</sub> ) <sub>4</sub> ]	Butterfly	$2.6 \times 10^{-11}$	$5 \times 10^{-17}$	$1.2 \times 10^{-10}$	$7.4 \times 10^{-5a}$	5(c)
[Et <sub>4</sub> N] <sub>3</sub> [MoOS <sub>3</sub> (CuBr) <sub>3</sub> (μ-Br)]	Half-open cubane-like	$1.6 \times 10^{-10}$	$-2.3 \times 10^{-16}$	$5.4 \times 10^{-10}$	$1.9 \times 10^{-3a}$	6(b)
[Et <sub>4</sub> N] <sub>3</sub> [WOS <sub>3</sub> (CuBr) <sub>3</sub> (μ-Br)]	Half-open cubane-like	$6.0 \times 10^{-10}$	$1.1 \times 10^{-16}$	$2.6 \times 10^{-10}$	$9.1 \times 10^{-4a}$	8(a)
[MoOS <sub>3</sub> Cu <sub>3</sub> I(py) <sub>5</sub> ]	Nest	$6.5 \times 10^{-10}$	$-3.0 \times 10^{-17}$	$7.5 \times 10^{-11}$	$2 \times 10^{-4a}$	5(a)
[WOS <sub>3</sub> Cu <sub>3</sub> I(py) <sub>5</sub> ]	Nest	$3.5 \times 10^{-10}$	$3.2 \times 10^{-17}$	$7.9 \times 10^{-11}$	$1.7 \times 10^{-4b}$	5(a)
[Et <sub>4</sub> N] <sub>4</sub> [Mo <sub>2</sub> O <sub>2</sub> S <sub>6</sub> Cu <sub>6</sub> I <sub>6</sub> ]	Twin-nest	$4 \times 10^{-10}$	$-6 \times 10^{-17}$	$1.6 \times 10^{-10}$	$2 \times 10^{-3a}$	9(a)
[MoOS <sub>3</sub> Cu <sub>3</sub> (PPh <sub>3</sub> ) <sub>3</sub> ]{S <sub>2</sub> P(OBu) <sub>2</sub> }	Cubane-like	$5 \times 10^{-10}$	$<10^{-19}$	$2 \times 10^{-11}$	$1.0 \times 10^{-4b}$	10(b)
[MoS <sub>4</sub> Cu <sub>2</sub> Ag(PPh <sub>3</sub> ) <sub>3</sub> Br]	Cubane-like	$8 \times 10^{-10}$	$3.8 \times 10^{-16}$	$4.5 \times 10^{-10}$	$4.5 \times 10^{-4a}$	28
[Mo <sub>2</sub> Ag <sub>4</sub> S <sub>8</sub> (PPh <sub>3</sub> ) <sub>4</sub> ]	Hexagonal prism	$1.8 \times 10^{-9}$	$2.2 \times 10^{-16}$	—	$1.3 \times 10^{-4c}$	6(a)
[W <sub>2</sub> S <sub>8</sub> Ag <sub>4</sub> (AsPh <sub>3</sub> ) <sub>4</sub> ]	Hexagonal prism	$7.8 \times 10^{-9}$	$5.9 \times 10^{-17}$	$1.7 \times 10^{-10}$	$1.3 \times 10^{-4a}$	5(b)
[n-Bu <sub>4</sub> N] <sub>4</sub> [Mo <sub>8</sub> Cu <sub>12</sub> O <sub>8</sub> S <sub>24</sub> ]	Twenty-nuclear cage	$2.3 \times 10^{-9}$	$-3.5 \times 10^{-16}$	$8.2 \times 10^{-10}$	$8.0 \times 10^{-4b}$	2(b)
[MoAu <sub>2</sub> S <sub>4</sub> (AsPh <sub>3</sub> ) <sub>2</sub> ]	Linear	$5.1 \times 10^{-10}$	$-5.1 \times 10^{-17}$	—	$6.4 \times 10^{-4b}$	7(b)
[WAu <sub>2</sub> S <sub>4</sub> (AsPh <sub>3</sub> ) <sub>2</sub> ]	Linear	$7.0 \times 10^{-10}$	$1.0 \times 10^{-16}$	—	$5.4 \times 10^{-4b}$	7(b)
{[MoOS <sub>3</sub> Cu <sub>3</sub> (CN)(py) <sub>3</sub> ]}·0.5C <sub>6</sub> H <sub>6</sub> } <sub>n</sub>	One-dimensional chain polymer	$5 \times 10^{-11}$	$-8 \times 10^{-18}$	—	$5.3 \times 10^{-5a}$	11(a)
[n-Bu <sub>4</sub> N][MoS <sub>4</sub> TI]	One-dimensional chain polymer	$2.2 \times 10^{-7}$	$3.1 \times 10^{-14}$	—	$5.1 \times 10^{-4a}$	12(d)
[n-Bu <sub>4</sub> N][WS <sub>4</sub> TI]	One-dimensional chain polymer	$1.8 \times 10^{-7}$	$3.2 \times 10^{-14}$	—	$4.9 \times 10^{-4a}$	12(d)
[MoS <sub>4</sub> Cu <sub>6</sub> I <sub>4</sub> (py) <sub>4</sub> ] <sub>n</sub>	Two-dimensional network polymer	$1.5 \times 10^{-9}$	$-2.5 \times 10^{-17}$	—	$6.5 \times 10^{-5d}$	15
{[Et <sub>4</sub> N] <sub>2</sub> [MoS <sub>4</sub> Cu <sub>4</sub> (CN) <sub>4</sub> ]} <sub>n</sub>	Three-dimensional framework polymer	$1.5 \times 10^{-9}$	$1.84 \times 10^{-16}$	$4.58 \times 10^{-9}$	$3.64 \times 10^{-5e}$	This work
{[Et <sub>4</sub> N] <sub>2</sub> [WS <sub>4</sub> Cu <sub>4</sub> (CN) <sub>4</sub> ]} <sub>n</sub>	Three-dimensional framework polymer	$1.6 \times 10^{-9}$	$1.22 \times 10^{-16}$	$5.12 \times 10^{-9}$	$2.93 \times 10^{-5e}$	This work

<sup>a</sup> In CH<sub>3</sub>CN. <sup>b</sup> In CH<sub>2</sub>Cl<sub>2</sub>. <sup>c</sup> In acetone. <sup>d</sup> In DMSO. <sup>e</sup> In DMF.

**Table 5** The limiting thresholds of compounds measured at 532 nm with ns laser pulses

Compound	Solvent	Linear transmission (%)	Limiting threshold/J cm <sup>-2</sup>	Ref.
C <sub>60</sub>	Toluene	60	1.6	29
[Bu <sub>4</sub> N] <sub>3</sub> [WCu <sub>3</sub> Br <sub>4</sub> S <sub>4</sub> ]	MeCN	70	1.1	7(a), 10(c)
[Bu <sub>4</sub> N] <sub>3</sub> [WAg <sub>3</sub> Br <sub>4</sub> S <sub>4</sub> ]	MeCN	70	0.6	7(a), 10(c)
[Bu <sub>4</sub> N] <sub>3</sub> [MoAg <sub>3</sub> Br <sub>4</sub> S <sub>4</sub> ]	MeCN	70	0.5	2(a)
Phthalocyanine derivatives	Toluene	85	0.1	30
[Mo <sub>2</sub> Ag <sub>4</sub> S <sub>8</sub> (PPh <sub>3</sub> ) <sub>4</sub> ]	MeCN	92	0.1	6(a), 7(d)
[MoS <sub>4</sub> Cu <sub>6</sub> I <sub>4</sub> (py) <sub>4</sub> ] <sub>n</sub>	DMSO	—	0.6	15
{[Et <sub>4</sub> N] <sub>2</sub> [MoS <sub>4</sub> Cu <sub>4</sub> (CN) <sub>4</sub> ]} <sub>n</sub>	DMF	70	0.28	This work
{[Et <sub>4</sub> N] <sub>2</sub> [WS <sub>4</sub> Cu <sub>4</sub> (CN) <sub>4</sub> ]} <sub>n</sub>	DMF	70	0.15	This work

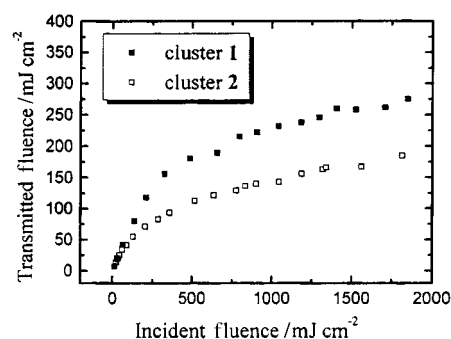


**Fig. 7** Optical limiting effect of {[Et<sub>4</sub>N]<sub>2</sub>[MoS<sub>4</sub>Cu<sub>4</sub>(CN)<sub>4</sub>]}<sub>n</sub> **1** ( $3.64 \times 10^{-5}$  mol dm<sup>-3</sup> in DMF) and {[Et<sub>4</sub>N]<sub>2</sub>[WS<sub>4</sub>Cu<sub>4</sub>(CN)<sub>4</sub>]}<sub>n</sub> **2** ( $2.93 \times 10^{-5}$  mol dm<sup>-3</sup> in DMF) at 532 nm.

clusters in the samples and  $F^4$  the local field correction factor. The  $\gamma$  values obtained for cluster polymers **1** and **2** are large, and comparable with those of related homologous clusters and other known NLO chromophores measured at 532 nm ( $1.6 \times 10^{-28}$  esu for a half-open cubane-like cluster [WOS<sub>3</sub>(CuBr)<sub>3</sub>(μ-Br)]<sup>3-</sup>,  $4.8 \times 10^{-29}$  esu for a nest-shaped cluster [MoOS<sub>3</sub>(CuNCS)<sub>3</sub>]<sup>2-</sup>,  $9 \times 10^{-29}$  esu for a butterfly-shaped cluster [WOS<sub>3</sub>Cu<sub>2</sub>(PPh<sub>3</sub>)<sub>4</sub>]<sup>5c</sup>,  $5.7 \times 10^{-28}$  esu for a supra-cage-shaped cluster [Mo<sub>8</sub>Cu<sub>12</sub>O<sub>8</sub>S<sub>24</sub>]<sup>4-</sup>,  $3.3 \times 10^{-32}$  esu for *trans*-[Mo(CO)<sub>4</sub>(PPh<sub>3</sub>)<sub>2</sub>] and  $1.7 \times 10^{-31}$  esu for *cis*-[Mo(CO)<sub>4</sub>(PPh<sub>3</sub>)<sub>2</sub>]<sup>23</sup> and at longer wavelengths ( $4.87 \times 10^{-29}$  esu for [Ru(dmb)<sub>2</sub>(PNOP)]<sup>+</sup> at 540 nm {dmb = 4,4'-dimethyl-2,2'-bipyridine; PNOP = 2(4-nitrophenyl)imidazo[4,5-*f*][1,10]phenanthroline}<sup>24</sup>,  $5.6 \times 10^{-35}$ – $8.6 \times 10^{-34}$  esu for Group 10 metal alkynyl polymers at 1064 nm,<sup>25</sup>  $1.0 \times 10^{-32}$ – $1.0 \times 10^{-31}$  esu for metallophthalocyanines at 1064 nm,<sup>26</sup> and  $7.5 \times 10^{-34}$  esu for C<sub>60</sub> and  $1.3 \times 10^{-33}$  esu for C<sub>70</sub>, both at 1910 nm<sup>27</sup>).

Based on the discussions above, we can reasonably state that cluster polymers **1** and **2** have similar NLO properties. Both exhibit strong non-linear absorption and self-focusing performance as exhibited in Figs. 5 and 6. It is also interesting to compare the optical non-linearities of these two cluster polymers with those of other different structural clusters or cluster polymers; the values  $a_2$ ,  $n_2$  and  $\chi^{(3)}$  of these clusters are listed in Table 4. The NLO refractive properties and NLO absorptive properties of **1** and **2** may be compared to the combined behaviors of the nest-shaped clusters and the cubane-like shaped clusters, which typically show effective self-focusing and strong non-linear absorption effects respectively.

The presence of combination effects of strong non-linear absorption and self-focusing in cluster polymers **1** and **2** may significantly enhance their overall optical limiting performance. The OL effects are depicted in Fig. 7. At very low fluence they respond linearly to the incident fluence, obeying Beer's law. The light transmittance starts to deviate from Beer's law when the input light fluence rises to certain values with respect to each cluster, and the solution become increasingly less transparent. Experiments with DMF solvents alone afforded no detectable OL effect. This indicates that the solvent contribution is negligible. The values of limiting threshold, which is defined as the incident fluence at which the actual transmittance falls to 50% of the corresponding linear transmittance, were measured as 0.28 and 0.15 J cm<sup>-2</sup> for clusters **1** and **2** separately from the OL experimental data.

Table 5 lists a few heterothiometallic clusters with their limiting thresholds. From the perspective of OL application, the present two cluster polymers with three-dimensional open frameworks are comparable to (or slightly better than) the known good optical limiting materials, cubane-like shaped clusters. Within a limited number of series of clusters where

both the W- and Mo-containing clusters are measured such a comparison can be made. The W-containing clusters seem always able to outperform their corresponding Mo-containing counterparts in OL performance at a given wavelength and with similar linear transmittance. This is consistent with the case that the OL effects of Ag-containing clusters are better than their Cu-containing homologues, which may due to the heavy-atom effect.<sup>7a</sup> In fact, cluster polymers possess the combined strength of both clusters and polymers, and exhibit very good NLO properties. The current work shows that constructing such molecules with extended structure is perhaps a promising research direction in the search for better NLO materials. Studies are underway to probe the NLO mechanism of these cluster polymers, and to design and prepare better materials with stronger NLO effects and applicable OL properties.

## Acknowledgements

This project was supported by the National Science Foundation (No. 29631040), Foundation of Harbin Institute of Technology, the Malaysian Government and Universiti Sains Malaysia (research grant R&D No. 190-9609-2801). The authors greatly thank Professors Dr Z. J. Guo, Dr L. M. Zheng and Dr C. Y. Duan for beneficial discussions.

## References

- E. I. Stiefel and K. Matsumoto (Editors), *Transition Metal Sulfur Chemistry: Biological and Industrial Significance*, American Chemical Society, Washington, DC, 1996; I. G. Dance and K. Fisher, *Prog. Inorg. Chem.*, 1994, **41**, 637; S. C. Lee and R. H. Holm, *Angew. Chem., Int. Ed. Engl.*, 1990, **29**, 840.
- (a) S. Shi, W. Ji, S. H. Tang, J. P. Lang and X. Q. Xin, *J. Am. Chem. Soc.*, 1994, **116**, 3615; (b) S. Shi, W. Ji and X. Q. Xin, *J. Phys. Chem.*, 1995, **99**, 894; (c) P. E. Hoggard, H. W. Hou, X. Q. Xin and S. Shi, *Chem. Mater.*, 1996, **8**, 2218; (d) M. K. M. Low, H. W. Hou, H. G. Zheng, W. T. Wong, G. X. Jin, X. Q. Xin and W. Ji, *Chem. Commun.*, 1998, 505.
- J. B. Howard and D. J. Low, *Chem. Rev.*, 1996, **96**, 2965; R. H. Holm, *Adv. Inorg. Chem.*, 1992, **38**, 1; D. Coucouvanis, *Acc. Chem. Res.*, 1991, **24**, 1; T. Shibahara, *Coord. Chem. Rev.*, 1993, **123**, 73; B. C. Wiegand and C. M. Friend, *Chem. Rev.*, 1992, **92**, 491.
- A. Muller, E. Diemann and H. Bogge, *Angew. Chem., Int. Ed. Engl.*, 1981, **20**, 934; H. W. Hou, X. Q. Xin and S. Shi, *Coord. Chem. Rev.*, 1996, **153**, 25; S. Sarkar and S. B. S. Mishra, *Coord. Chem. Rev.*, 1984, **59**, 239; J. Guo, X. T. Wu, W. J. Zhang, T. L. Sheng, Q. Huang, P. Lin, Q. M. Wang and J. X. Lu, *Angew. Chem., Int. Ed. Engl.*, 1997, **36**, 2464.
- (a) P. Ge, S. H. Tang, W. Ji, S. Shi, H. W. Hou, D. L. Long, X. Q. Xin, S. F. Lu and Q. J. Wu, *J. Phys. Chem. B*, 1997, **101**, 27; (b) G. Sakane, T. Shibahara, H. W. Hou, X. Q. Xin and S. Shi, *Inorg. Chem.*, 1995, **34**, 4785; (c) S. Shi, H. W. Hou and X. Q. Xin, *J. Phys. Chem.*, 1995, **99**, 4050.
- (a) W. Ji, S. Shi, H. J. Du, P. Ge, S. H. Tang and X. Q. Xin, *J. Phys. Chem.*, 1995, **99**, 17297; (b) S. Shi, Z. R. Chen, H. W. Hou, X. Q. Xin and K. B. Yu, *Chem. Mater.*, 1995, **7**, 1519; (c) S. Shi, W. Ji, W. Xie, T. C. Chong, H. C. Zeng, J. P. Lang and X. Q. Xin, *Mater. Chem. Phys.*, 1995, **39**, 298.
- (a) S. Shi, W. Ji, J. P. Lang and X. Q. Xin, *J. Phys. Chem.*, 1994, **98**, 3570; (b) H. G. Zheng, W. Ji, M. K. M. Low, G. Sakane, T. Shibahara and X. Q. Xin, *J. Chem. Soc., Dalton Trans.*, 1997, 2357; (c) H. G. Zheng, W. L. Tan, W. Ji, W. H. Leung, I. D. Williams, D. L. Long, J. S. Huang and X. Q. Xin, *Inorg. Chim. Acta*, 1999, **294**, 73; (d) T. Xia, A. Dogariu, K. Mansour, D. J. Hagan, A. A. Said, E. W. Van Stryland and S. Shi, *J. Opt. Soc. Am. B*, 1998, **15**, 1497.
- (a) Z. R. Chen, H. W. Hou, X. Q. Xin, K. B. Yu and S. Shi, *J. Phys. Chem.*, 1995, **99**, 8717; (b) H. W. Hou, B. Liang, X. Q. Xin, K. B. Yu, P. Ge, W. Ji and S. Shi, *J. Chem. Soc., Faraday Trans.*, 1996, 2343; (c) D. X. Zeng, W. Ji, W. T. Wong, W. Y. Wong and X. Q. Xin, *Inorg. Chim. Acta*, 1998, **279**, 172.
- (a) H. W. Hou, D. L. Long, X. Q. Xin, X. Y. Huang, B. S. Kang, P. Ge, W. Ji and S. Shi, *Inorg. Chem.*, 1996, **35**, 5363; (b) H. W. Hou, X. Q. Xin, J. Liu, M. Q. Chen, S. Shi, *J. Chem. Soc., Dalton Trans.*, 1994, 3211.
- (a) H. W. Hou, X. R. Ye, X. Q. Xin, J. Liu, M. Q. Chen and S. Shi, *Chem. Mater.*, 1995, **7**, 472; (b) D. L. Long, S. Shi, X. Q. Xin, B. S. Luo, L. R. Chen, X. Y. Huang and B. S. Kang, *J. Chem. Soc., Dalton Trans.*, 1996, 2617; (c) W. Ji, H. J. Du, S. H. Tang and S. Shi, *J. Opt. Soc. Am. B*, 1995, **12**, 876.
- (a) H. W. Hou, H. G. Zheng, H. G. Ang, Y. T. Fan, M. K. M. Low, Y. Zhu, W. L. Wang, X. Q. Xin, W. Ji and W. T. Wong, *J. Chem. Soc., Dalton Trans.*, 1999, 2953; (b) Q. Huang, X. T. Wu, Q. M. Wang, T. L. Sheng and J. X. Lu, *Angew. Chem., Int. Ed. Engl.*, 1996, **35**, 868; (c) Q. Huang, X. T. Wu and J. X. Lu, *Inorg. Chem.*, 1996, **35**, 7445; (d) Q. Huang, X. T. Wu and J. X. Lu, *Chem. Commun.*, 1997, 703; (e) H. Yu, W. J. Zhang, X. T. Wu, T. L. Sheng, Q. M. Wang and P. Lin, *Angew. Chem., Int. Ed.*, 1998, **37**, 2520.
- (a) J. P. Lang, S. A. Bao, X. Q. Xin and K. B. Yu, *Polyhedron*, 1993, **12**, 801; (b) A. Muller, W. Jaegermann and W. Hellmann, *J. Mol. Struct.*, 1983, **100**, 559; (c) Q. Huang, X. T. Wu, T. L. Sheng and Q. M. Wang, *Inorg. Chem.*, 1995, **34**, 4931; (d) J. P. Lang, K. Tatsumi, H. Kawaguchi, J. M. Lu, P. Ge, W. Ji and S. Shi, *Inorg. Chem.*, 1996, **35**, 7924; (e) J. P. Lang, J. Liu, M. Q. Chen, J. M. Lu, G. Q. Bian and X. Q. Xin, *J. Chem. Soc., Chem. Commun.*, 1994, 2665.
- J. M. Manoli, C. Potvin, F. Secheresse and S. Marzak, *Inorg. Chim. Acta*, 1988, **44**, 170.
- J. R. Nicholson, A. C. Flood, C. D. Garner and W. Clegg, *J. Chem. Soc., Chem. Commun.*, 1983, 1179; C. Potvin, J. M. Manoli, F. Secheresse and S. Marzak, *Inorg. Chem.*, 1987, **26**, 4370; J. M. Manoli, C. Potvin, F. Secheresse and S. Marzak, *J. Chem. Soc., Chem. Commun.*, 1986, 1557; *Inorg. Chim. Acta*, 1988, **150**, 257.
- H. W. Hou, Y. T. Fan, C. X. Du, Y. Zhu, W. L. Wang, X. Q. Xin, M. K. M. Low, W. Ji and H. G. Ang, *Chem. Commun.*, 1999, 647.
- C. L. Bowes and G. A. Ozin, *Adv. Mater.*, 1996, **8**, 13; A. K. Cheetham, G. Ferey and T. Loiseau, *Angew. Chem., Int. Ed.*, 1999, **38**, 3269; P. J. Hargman, D. Hargman and J. Zubieta, *Angew. Chem., Int. Ed.*, 1999, **38**, 2638 and references therein.
- H. L. Li, A. Laine, M. O'Keeffe and O. M. Yaghi, *Science*, 1999, **283**, 1145; O. M. Yaghi, H. L. Li, C. Davis, D. Richardson and T. L. Groy, *Acc. Chem. Res.*, 1998, **31**, 474.
- J. W. McDonald, G. D. Frieson, L. D. Rosenhein and W. E. Newton, *Inorg. Chim. Acta*, 1983, **72**, 205.
- C. K. Johnson, ORTEP II, Report ORNL-5138, Oak Ridge National Laboratory, Oak Ridge, TN, 1976.
- Y. Jeannin, F. Secheresse, S. Bernes and F. Robert, *Inorg. Chim. Acta*, 1992, **198–200**, 493; A. Muller, M. Dartmann, C. Romer, W. Clegg and G. M. Sheldrick, *Angew. Chem., Int. Ed. Engl.*, 1981, **20**, 1060; S. F. Gheller, T. W. Hambley, J. R. Rodgers, R. T. C. Brownlee, M. J. O'Conner, M. R. Snow and A. W. Wedd, *Inorg. Chem.*, 1984, **23**, 2519; S. R. Actt, C. D. Garner, J. R. Nicholson and W. Clegg, *J. Chem. Soc., Dalton Trans.*, 1983, 713; M. Minelli, J. H. Enemark, J. R. Nicholson and C. D. Garner, *Inorg. Chem.*, 1984, **23**, 4384.
- (a) J. R. Nicholson, A. C. Flood, C. D. Garner and W. Clegg, *J. Chem. Soc., Chem. Commun.*, 1983, 1179; (b) C. Potvin, J. M. Manoli, F. Secheresse and S. Marzak, *Inorg. Chem.*, 1987, **26**, 4370; (c) J. M. Manoli, C. Potvin, F. Secheresse and S. Marzak, *J. Chem. Soc., Chem. Commun.*, 1986, 1557; (d) J. M. Manoli, C. Potvin, F. Secheresse and S. Marzak, *Inorg. Chim. Acta*, 1988, **150**, 257.
- (a) M. Sherk-Bahae, A. A. Said, T. H. Wei, D. J. Hagan and E. W. Van Stryland, *IEEE J. Quantum Electron.*, 1990, **26**, 760; (b) M. Sherk-Bahae, A. A. Said and E. W. Van Stryland, *Opt. Lett.*, 1989, **14**, 955; (c) A. A. Said, M. Sherk-Bahae, D. J. Hagan, T. H. Wei, J. Wang, J. Young and E. W. Van Stryland, *J. Opt. Soc. Am. B*, 1992, **9**, 405.
- T. Zhai, C. M. Lawson, D. C. Gale and G. M. Gray, *Opt. Mater.*, 1995, **4**, 455.
- H. Chao, R. H. Li, B. H. Ye, H. Li, X. L. Feng, J. W. Cai, J. Y. Zhou and L. N. Ji, *J. Chem. Soc., Dalton Trans.*, 1999, 3711.
- S. Guha, C. C. Frazier, P. L. Porter, K. Kang and S. E. Finberg, *Opt. Lett.*, 1989, **14**, 952; W. J. Blau, H. J. Byrne, D. J. Cardin and A. P. Davey, *J. Mater. Chem.*, 1991, **1**, 245.
- J. S. Shirk, J. R. Lindley, F. J. Bartoli, Z. H. Kafafi and A. W. Snow, in *Materials for Nonlinear Optics*, eds. S. R. Marder, J. E. Sohn and G. D. Stucky, American Chemical Society, Washington, 1992, p. 626.
- Y. Wang and L. T. Cheng, *J. Phys. Chem.*, 1992, **96**, 1530.
- D. L. Long, Ph.D. Dissertation, Nanjing University, 1996.
- D. G. McLean, R. L. Sutherland, M. C. Brant, D. M. Brandelik, P. A. Fleitz and T. Pottenger, *Opt. Lett.*, 1993, **18**, 858.
- J. W. Perry, K. Mansour, S. R. Marder, K. J. Perry, D. Alvarez, Jr. and L. Choong, *Opt. Lett.*, 1994, **19**, 625; J. W. Perry, K. Mansour, I. Y. S. Lee, X. L. Wu, P. V. Bedworth, C. T. Chen, D. Ng, S. R. Marder, P. Miles, T. Wada, M. Tian and H. Sasabe, *Science*, 1996, **273**, 1553.
- G. M. Sheldrick, SADABS, Empirical absorption correction program, University of Gottingen, 1997.
- G. M. Sheldrick, SHELXTL-PC (version 5.1), Siemens Analytical Instruments, Inc., Madison, WI, 1997.